



UNIVERSITY OF LEEDS

This is a repository copy of *Vacuum drying of advanced gas reactor fuel*.

White Rose Research Online URL for this paper:

<http://eprints.whiterose.ac.uk/142262/>

Version: Accepted Version

Article:

Goode, JB, Harbottle, D orcid.org/0000-0002-0169-517X and Hanson, BC orcid.org/0000-0002-1720-1656 (2018) Vacuum drying of advanced gas reactor fuel. *Progress in Nuclear Energy*, 109. pp. 145-158. ISSN 0149-1970

<https://doi.org/10.1016/j.pnucene.2018.07.011>

(c) 2018, Elsevier Ltd. This manuscript version is made available under the CC BY-NC-ND 4.0 license <https://creativecommons.org/licenses/by-nc-nd/4.0/>

Reuse

This article is distributed under the terms of the Creative Commons Attribution-NonCommercial-NoDerivs (CC BY-NC-ND) licence. This licence only allows you to download this work and share it with others as long as you credit the authors, but you can't change the article in any way or use it commercially. More information and the full terms of the licence here: <https://creativecommons.org/licenses/>

Takedown

If you consider content in White Rose Research Online to be in breach of UK law, please notify us by emailing eprints@whiterose.ac.uk including the URL of the record and the reason for the withdrawal request.



eprints@whiterose.ac.uk
<https://eprints.whiterose.ac.uk/>

Vacuum Drying of Advanced Gas Reactor Fuel

James B. Goode^a, David Harbottle^a, Bruce C. Hanson^{a,*}

^a*School of Chemical and Process Engineering, University of Leeds, Leeds, LS2 9JT*

Abstract

The UK will shortly cease reprocessing spent advanced gas reactor (AGR) fuel in favour of direct disposal, however since a permanent geological disposal facility is not envisaged as being available until 2075 interim storage will be required. The initial intention is to continue wet storage but it is possible that this may not be viable for as long as is hoped. Dry storage is commonly used worldwide for the interim storage of zirconium clad spent nuclear fuel however AGR fuel is stainless steel (SS) clad and as such a new safety case will be required to ensure that fuel can be adequately and safely dried.

A rig has been designed to allow a comparison of the two main drying techniques in use; vacuum drying and flowed gas drying. This paper looks primarily at the design and development of the rig. Some of the initial data is presented to indicate how the rig was developed as a result of early results and is followed by some of the later test data to illustrate the improvements made.

Keywords: nuclear fuel, dry storage, stainless steel, AGR

1. Introduction

In 1956 the United Kingdom opened Calder Hall the worlds first commercial nuclear power plant. The Calder Hall plant utilised a graphite core as the moderator, natural uranium fuel and pressurised carbon dioxide as the coolant with the name, Magnox, being derived from Magnesium Non-Oxidising in reference to the special magnesium alloy used for the fuel cladding. The design was very similar to the first reactors built in France, the UNGG (Uranium Naturel Graphite Gaz) with the key difference being the use of a magnesium-zirconium alloy for the cladding. When the second generation of reactors were being designed the CEA and Framatome changed course with France now developing water cooled and moderated reactors which had initially been developed by GE and Westinghouse in the United States, while the British continued with gas cooled reac-

tors developing what is known as the Advanced Gas-cooled Reactor or AGR.

Like Magnox, AGR reactors were graphite moderated and carbon dioxide cooled however the thermal efficiency of the reactor was increased from 32% to 45% by increasing the coolant temperature at the outlet (and in turn the steam temperature) from 370°C to 650°C [1]. In order to deal with the increased temperatures metallic uranium was replaced with ceramic uranium dioxide and magnesium alloy cladding was replaced with stainless steel (SS).

In order to prevent radiolytic oxidation of the graphite core by the carbon dioxide coolant corrosion inhibitors were used. In the early Magnox reactors the addition of carbon monoxide was sufficient however as the coolant pressure was increased in the later Magnox reactors it was found that hydrogen was more effective. The AGR's required yet another change and the addition of small quantities of methane was adopted alongside carbon monoxide and water[2]. Unfortunately the use of inhibitors leads to carbon deposits on metal surfaces such as fuel cladding leading to

*Corresponding author

Email address: B.C.Hanson@Leeds.ac.uk (Bruce C. Hanson)

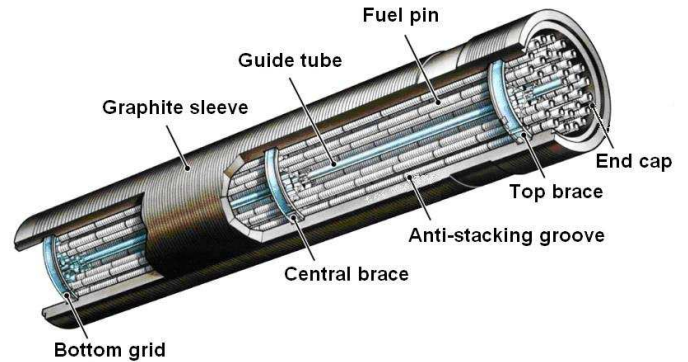
a reduction in heat transfer, however to prevent
45 core damage such deleterious effects must be ac-
cepted.

A fuel element used in the AGR reactors is
shown in fig. 1a. Each element consists of thirty
six pins held together by SS grids and surrounded
50 by a graphite sleeve. A SS tie bar is threaded
through the guide tube of eight elements (seven
in the case of Dungeness B) to produce what is
known as a stringer and these are in turn low-
ered into one of 308 channels in the graphite core
55 [2]. Each pin is approximately 1 m in length and
15.5 mm in diameter. The pins are manufactured
from 20wt% Cr, 25wt% Ni and 2wt% Nb stainless
steel[3] and are machined to form grooves on the
surface to increase heat flow leaving a wall thick-
60 nesses of 400 μm . The fuel pellets are annular
with an outside diameter of around 14.5 mm and an
inner diameter 6.4 mm. The pellets are fed into
the pins, which are backfilled with helium and end
caps are welded in place. Following welding the
65 pins are annealed in hydrogen at 980°C.

Following irradiation and removal from the core
the spent nuclear fuel (SNF) is initially held in
cooling ponds at the reactors for a short period,
typically six month (based on the safety case for
70 fuel acceptance) before being transferred to Sell-
afield for reprocessing. Upon arrival at Sellafield
the graphite sleeve is removed and the individual
pins are removed from the grids. The pins from
three elements are placed into a slotted can and
75 then transferred to cool before reprocessing.

The cooling ponds at Sellafield were initially
filled with demineralised water, however in the
early years of operation (from 1978) it was found
that failures were taking place (see fig. 2)[5] lead-
80 ing to the release of soluble caesium and other
radionuclides. An investigation into this found
that such failures were due to intergranular attack
(IGA) combined with stresses within the cladding
leading to intergranular stress corrosion cracking
85 (IGSCC) and that in demineralised water failures
would occur within 200 days [5].

IGA normally occurs due to thermal sensiti-
sation, when chromium carbides form at grain
boundaries leading to localised chromium deple-
90 tion, leaving the SS more susceptible to corrosion[6].



(a) AGR fuel element.



(b) Slotted can

Figure 1: An AGR fuel element and slotted can (taken from [4]).

In AGR fuel cladding the niobium is present to ef-
fectively mop up carbon by preferentially forming
niobium carbides thus preventing chromium car-
bide formation and chromium depletion. Conse-
quently chromium depletion in AGR fuel cladding
is attributed to radiation induced segregation (RIS)[7].
RIS is the diffusion of an element, in this case
chromium, against the concentration gradient when
in the presence of radiation[8, 9] and has been
found to be most serious between 400°C and 420°C
[10]. Temperatures in this range are experienced
by the cladding of the first two elements on each
stringer (at the base of the core) [11] and in test-

ing 50% of pins from elements 1 and 2 were found
to fail by IGSCC[5, 4].

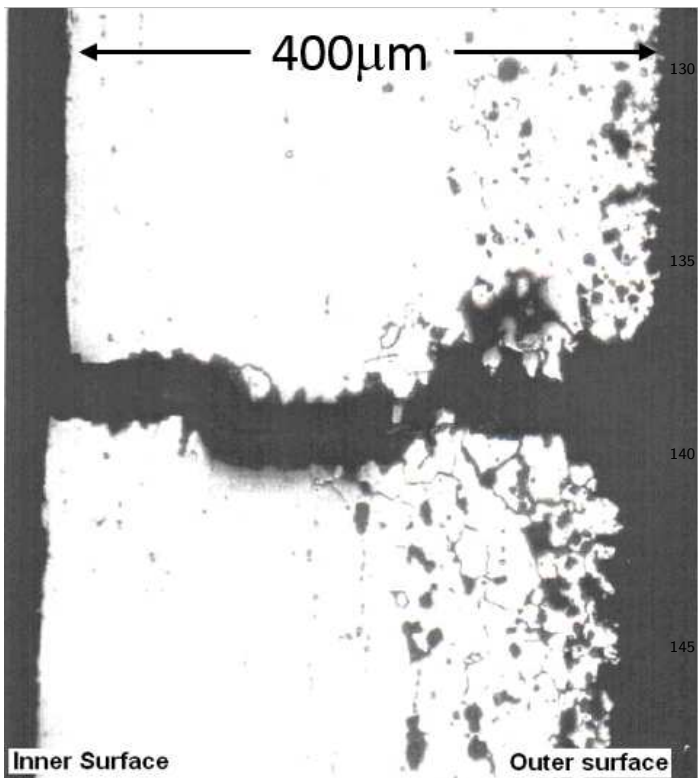


Figure 2: Failed cladding pre caustic dosing with significant IGA on the outer surface. The crack width is approximately $50 \mu m$ (taken from[4]).

In order to address this problem a series of corrosion tests were undertaken in the early 1980's to find a corrosion inhibitor and sodium hydroxide (caustic) was identified as most suitable[5]. This led to the dosing of the AGR storage pond to pH 11.4 since when there have been no reported failures. Up until 1993 post storage examination (PSE) was carried out regularly and found evidence of limited IGA [11]. Since then there has been only limited PSE and that has found no significant degradation beyond that found upon removal from the reactor[4].

In recent years the decision has been made by the Nuclear Decommissioning Authority (NDA) that reprocessing of AGR fuel will cease with the fuel being sent for direct disposal to a geological disposal facility (GDF). The expectation is that a GDF will not be available until 2075[12]. Sellafield Ltd intend to continue reprocessing until 2018 with future arisings being put into in-

terim storage. Operating experience has shown that fuel can be stored safely for 25 years if caustic conditions are maintained, however it is unknown how fuel behaves beyond this or whether the higher burnup fuels of recent and future years will be suitable for extended pond storage. Consequently Sellafield Ltd will try to extend pond storage beyond this time frame. If this is not possible a second option should be available and the next best option is dry storage.

When spent fuel is placed into storage, either wet or dry, the conditions must be controlled to prevent negative impacts on criticality, general containment of radionuclides, the ability to retrieve the fuel at the end of the storage period and final disposal options[13]. The geometry of fuel is such that without a moderator, criticality is not possible, however in extreme cases when temperatures escalate there is a minor chance of criticality due to changes in fuel geometry due to creep. Such changes may also lead to cladding damage releasing otherwise contained radionuclides, or a change in shape that prevents fuel being removed from whatever storage container has been used or makes the final disposal option non viable.

Similarly corrosion can lead to failure of the cladding and radionuclide release, or in extreme cases geometry changes. Equally the final form may no longer be suitable for the disposal option or corrosion may lead to the formation of potentially dangerous corrosion products, such as hydrogen gas or uranium hydride which complicate recovery[14].

The impacts of creep and other temperature related issues can be negated almost entirely by water storage since the water carries away decay heat. Water will at the same time provide shielding and trap released radionuclides which can be later removed by filtration. While water can be somewhat corrosive, careful control of water chemistry means that corrosion can be held in check for significant lengths of time with some AGR fuel having been stored without failure since 1986[11]. Water storage does however require ongoing monitoring and continual control which impacts running costs and there are limits to the quantity of fuel a pond can hold before it has

reached capacity.

When the United States stopped reprocessing nuclear fuel in 1976 the expectation was that the government would provide a repository for spent fuel disposal however over forty years later such a facility is still not available. As ponds reached capacity this led to the development of dry stores with the first being licensed in 1986[15]. The basic concept of dry storage is to place the fuel in a sealed canister which provides the shielding from radiation and contains any released radionuclides

Sindelar et al.[13] have described dry storage existing as either unsealed or sealed systems. In an unsealed system fuel is generally placed into a concrete vault or silo through which gas can flow to provide cooling and allows monitoring of the fuel condition, however the need to do this increases the costs and sealed systems are the preferred option. As the name suggests in a sealed system the fuel is sealed inside a cask with the expectation that it will remain there until final disposal. Being a sealed system means that it is difficult to remove decay heat and as such these systems are not suitable for fuel that has not undergone several years pond cooling, however such systems require no ongoing monitoring, are modular in nature and as such can be increased in size as required with the addition of new casks. However the risks of degradation are heightened as the presence of only a small amount of water in a potentially hot, sealed, radioactive environment can lead to the formation of various aggressive species such as hydrogen and hydroxide radicals, and hydrogen peroxide[16]. As such the drying of spent fuel prior to loading is of critical importance. In the United States dry storage of SNF has been carried out for many years prior to which significant experimentation was undertaken to establish a safety case for all aspects of dry storage and this has led to the development of ASTM C-1553 A Standard Guide for Drying Behaviour of SNF[17]. The standard identifies two methods for drying SNF; vacuum drying and Forced Helium Dehydration. Various authors[18, 19, 20, 21, 22, 23, 24, 25] have presented work on vacuum drying using different parameters and fuels however it is not possible to make a comparison between these investi-

gations due to differences in the fuels being dried such as cladding material, fuel geometry, fuel form (metallic or ceramic fuel) and the presence (or not) of crud or organic materials. The forced helium dehydration method is patented by Holtec and while other companies use similar methods there is insufficient detail published as organisations are keen to protect their proprietary IP.

Whichever drying technique is used, dryness is confirmed with the use of a vacuum rebound test in which the sealed container is required to maintain a pressure of 3 torr ($\sim 4\text{mBarA}$) for at least 30 minutes. While a small amount of work has been conducted to try and match the dryness to a specific dew point this has as yet been unsuccessful[26].

While dry storage of spent fuel has been examined in significant detail, this work has been carried out almost exclusively on zirconium and aluminium clad fuels and it is not certain that the same safety case and drying techniques can be used for SS clad fuels. With dry storage being considered for future interim storage of AGR fuel it was felt necessary to begin to investigate dry storage in relation to SS clad AGR fuels. This paper looks at the development of a drying rig which is to be used to compare vacuum drying (VD) with flowed gas drying (FGD) methods such as Holtec's Forced Helium dehydration, and assess the impact of different gases on drying behaviour.

2. Drying Requirements

Dry storage of SNF is used as an interim storage option for fuel that has been previously pond stored to allow decay heat to reduce to an acceptable level. In the early days of dry storage fuel had often been stored for decades and as such had little decay heat but more recently hotter fuel has begun to go into dry storage. Whatever the age and decay heat of the fuel, the important point is that water must be reduced to a level low enough to prevent unacceptable levels of corrosion. A secondary requirement is to reduce the potential for hydrogen build up from radiolysis of water remaining in the cask during storage.

ASTM C-1553 identifies two forms of water

265 that are liable to be a concern; bound water specifically chemisorbed water and trapped water. Chemisorbed water is defined as being “water that is bound to other species by forces whose energy levels approximate those of a chemical bond” while³¹⁵
270 trapped water is defined as “unbound water that is physically trapped or contained by the surrounding matrix, blocked vent pores, cavities, or by the nearby formations of solids that prevent or slow escape”.

275 The presence of trapped water is a concern with two possibilities. One concern is the presence of water within the pore network of carbonaceous deposits and the danger posed by such water is being investigated elsewhere but is yet to³²⁵
280 be reported. Whatever the case, the second concern is expected to be more serious. For AGR fuel, the concern is a fuel pin that has become flooded. As described above the historical failures of AGR cladding were due to IGSCC. While
285 caustic dosing of the pond water appears to have stopped failures there is evidence of minor intergranular attack. Since the detection of failures is detected primarily through the measurement of the pond water caesium content there is a concern
290 that some pins may have micro cracks which are too small for caesium to be released in sufficient quantities for detection yet have allowed pins to become flooded over many decades under water. If such a pin was then placed into dry storage the trapped water may then be released.

295 Since there could eventually be millions of individual fuel pins it is not practical to analyse a sufficiently large sample to be able to rule out the possibility of a flooded pin and as such the presence of such a pin is regarded as the worst case,
300 but realistic possibility. In order to investigate whether it is possible to remove water through such cracks it was felt that an experimental rig³³⁰
305 would need to be constructed that would allow a direct comparison between vacuum and flowed gas drying. The remainder of this paper discusses the development of the rig and presents the initial data collected. It then discusses the changes³³⁵
310 and improvements that the initial data prompted and shows the data the rig and instrumentation is able to record and what that may indicate.

3. Experimental Setup

As described above the purpose of this work is to compare vacuum drying (VD) methods with flowed gas drying (FGD). To this end it was felt that a multi purpose drying rig would be required which would minimise the variations between systems. The following sections discuss the key parts of the rig. For VD the main requirements are a drying vessel and a vacuum pump. FGD is generally carried out by recirculating gas in a sealed system. Such a system is therefore much more complicated requiring a gas pump and heater in addition to the vessel as well as a method of drying the gas to be recirculated. Figure 3 shows the completed drying rig and fig. 4 shows the P&ID of the rig.

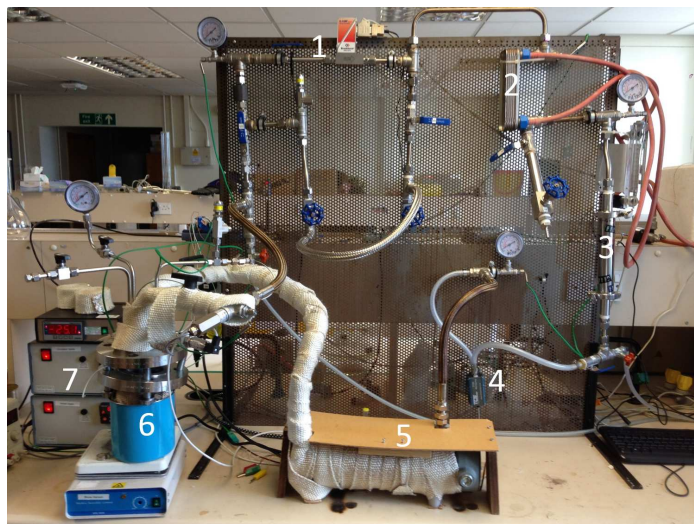


Figure 3: Latest iteration of the drying rig. 1-Flowmeter, 2-condenser, 3-molecular sieve, 4-circulation pump, 5-circulation heater, 6- drying vessel and 7-heater controller.

3.1. Drying Vessel

The system was developed around a single drying vessel (fig. 3). The vessel was constructed from a length of 2.5” 316 stainless steel pipe. A domed cap was welded to one end and a flange to the other. A blank flange was used as a lid with multiple lines fitted. One of the two main lines had a dip tube in place to allow a flow of gas from the bottom the vessel. Both an analogue pressure gauge (PG) and digital pressure transducer (PT)

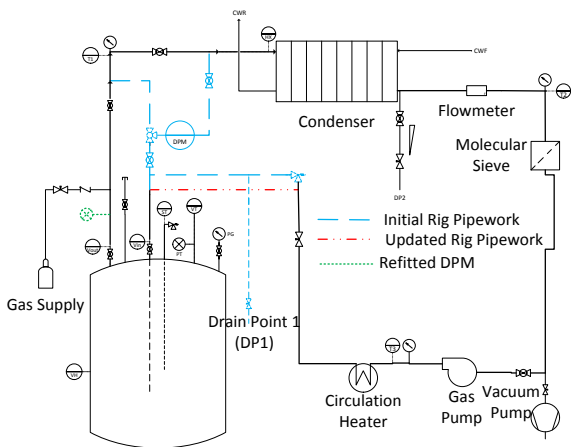


Figure 4: P&ID of the drying rig.

were fitted. Two Omega PXM319 pressure transducers were obtained; one with a 0-2 BarA range and the second with a 0-15 BarA range. One or other transducer was used depending upon the pressure being used. Two k-type thermocouples (TC) were fitted; one for recording the temperature of the gas in the vessel (VT) and a second flexible TC which could be attached to the surface of the object being dried (ST). The vessel was heated with a 4" Mineral Insulated band heater purchased from Watlow Ltd and then insulated. The band heater had an integrated TC which was used for temperature control (VH). Temperature controller was purchased (also from Watlow) and made into a temperature control unit in-house.

3.2. Gas Pump and Heater

For FGD a TCS D10K micropump was sourced which was designed to pump gas at a maximum flow rate of 11 l min^{-1} of air at atmospheric pressure with a differential pressure of 6 psi ($\sim 400 \text{ mBar}$). The pump was set to run at full power.

Gas heating was provided with a Cast-X 2000 240V, 1kW circulation heater. The control thermocouple was located at the inlet to the vessel (Vin). The circulation heater and controller were purchased from Watlow Ltd.

3.3. Gas Drying

A two stage gas drying system was utilised. The first stage was a water cooled condenser/plate

heat exchanger to remove the bulk water for conditions about the dew point while the second stage was a scrubber column packed with molecular sieve. The condenser was set up with a twin valve drain system so that bulk water could be removed while the system was in operation. The drying system was put in place primarily for FGD to ensure that dry gas was returned to the vessel but also played a role in protecting the vacuum pump from water vapour.

3.4. Further Instrumentation and Pipework

Numerous K-Type TC's were fitted around the rig in addition to those mentioned above to give a good temperature profile around the rig. The level of instrumentation was intended to give the operator a clear view of where water is present (and to what degree) in the rig during operation. These were placed at the vessel outlet (Vout), mid way to the condenser (T1), at the inlet to the condenser (HX), between the condenser and molecular sieve (T2) and between the pump and circulation heater (T3). T1, 2 and 3 all had analogue pressure gauges alongside. TC's were also fitted to the cooling water flow (CWf) and return (CW_r).

A Michell Easidew dew point meter (DPM) was fitted into the system. This had a range of -100°C to $+20^{\circ}\text{C}$. The system was designed such that when FGD operations were in operation gas could be fed to the DPM either directly from the heater to measure the dry gas dew point (DP) or from the vessel (wet gas). It was also possible to bypass the DPM when carrying out 150°C tests to avoid exceeding the DPM's operating temperature and damaging the instrument.

A Bronkhorst El-Flow mass flow meter (FM) was fitted in the line between the condenser and molecular sieve. It was specified using the maximum pump flow rate (11 l min^{-1}) and the maximum pressure that was expected to be used (11 BarA).

The major lines were constructed with 12 mm OD SS tube and 1/2" BSP SS fittings. The pipework between the circulation heater and vessel and the vessel and the condenser was all lagged and heat traced to prevent heat loss and minimise con-

densation prior to the dew point meter and condenser.

415 The system was initially designed to use mains water with an expected temperature of $<10^{\circ}\text{C}$ but was replaced with water at room temperature pumped from a tank since the mains water was found to be approaching 27°C .

420 3.5. Early Design and Operational Changes

When the design for the system was initially conceived the intention had been to mount the vessel onto a balance to allow real time measurement of mass loss. It was found that it was not possible to keep the vessel steady enough in oper-
425 ation for useful data to be collected and this was abandoned.

A 5g heel of water was placed into the vessel at the beginning of each test. This was to represent the water that will be left behind when bulk water
430 is pumped from a spent fuel cask.

The dew point meter which was fitted was found to be unsuitable. It was found that the humidity of the system quickly overwhelmed the DPM with two DPM's failing during commission-
435 ing. The use of a DPM was therefore abandoned and water loss determined primarily by mass loss from the TP with a mass balance using the mass change of the molecular sieve and condenser.

Perhaps the greatest challenge is the produc-
440 tion of samples for testing. In order for this to be possible the test piece (TP) must allow water to be sealed inside and yet be known to have cracks of an appropriate size. Early work to produce
445 such a sample suggests that this is possible how-
ever that work is ongoing. The trials discussed here were carried out with a TP containing a machined hole of $300\mu\text{m}$ diameter to simulate a pinhole.

450 4. Initial Drying Tests

Initial drying trials were carried out at three nominal pressures; 30 mBarA (vacuum), 1000 mBarA (ambient pressure, AP) and 11,000 mBarA (high pressure, HP). Three temperatures were used; room
455 temperature (RT) when no heat was supplied, 60°C and 150°C with the temperatures relating



Figure 5: The test piece. The pinhole is just visible as a small black dot in the area highlighted.

to the set point of the heater and were an approximation of the vessel wall temperature. For vacuum tests there was no gas flow. The AP and HP tests were FGD tests and the circulation heater was set to the same temperature as the vessel. In the initial tests different gases were also used; air, nitrogen, carbon dioxide and argon. This meant that a total of 36 different tests conditions were initially tested. Each test began with three cycles of evacuation followed by backfill with the test gas.

For each test the TP shown in fig. 5 was filled with 2-3 g of water. The TP is constructed from a SS plug welded into a short length of AGR fuel cladding with a pinhole drilled through it. A length of SS tube is welded into the other end a Swagelok cap fitted. The TP was weighed before and after each test. An overall drying rate was calculated for each test by dividing the mass change by the length of the test. The test duration was nominally 60 minutes for RT and 60°C tests. It was reduced to a nominal 30 minutes for the 150°C tests since a quantity of water needed to remain at the end of the test to allow a rate to be calculated. The work produced two main data outputs; a drying rate based on the rate of mass loss and a data plot based on instrumentation readings.

485 4.1. Vacuum Drying Plot

A typical data plot for a 150°C vacuum drying test is shown in fig. 6. The data in the bottom right hand corner shows the test ID and the overall drying rate. From the data in the plot it is possible to get an idea of what is happening within the system. Some of the events discussed are not visible in the plot due to the scale but are

discussed to provide an idea of what can be seen. Multiple large scale plots for fig. 6 are available in the addendum which shows these events.

0-300 seconds. The vessel begins the test at full temperature (150°C) and as such ST (TP surface temperature) begins relatively high as it has been warming in the delay between being placed in the vessel and the beginning of the test. The flow rate and pressure spike several times as the system undergoes gas flushes to replace the air in the system with the test gas, during which time ST and VT (vessel gas temperature) fluctuate. Following the gas flushes VT and ST drop due to adiabatic cooling as the pressure is reduced to vacuum conditions. VT levels out at 27°C. This is the boiling point of water at the vessel pressure of 37 mBarA suggesting the vessel is now full of saturated water vapour. The TP is sitting in a pool of water but is also in contact with the vessel walls so is warmed by conduction so the behaviour of ST changes somewhat during this period as the water level drops. As the water level drops ST begins to rise quicker than VT (the vessel gas temperature). Flow rate begins to rise around 200 s as the water begins to boil.

300-800 seconds. Around 300 s the heel water has been removed and VT begins to rise. There is a small drop in pressure and flow rate drops. After the drop in flow rate it begins to rise again as ST rises and greater quantities of water vapour are able to evaporate from inside the TP.

800-1200 seconds. Around 800 s the water in the TP begins to boil vigorously leading to sharp rises in flow rate and pressure and a change in the rate of change of ST as slugs of water are ejected through the pinhole. The sharp rises in flow and pressure are accompanied by spikes in CWout, T1 and HX as the greater mass of water vapour carries more heat.

1200-1300. Around 1200 s the water inside the TP appears to boil less vigorously. The belief is that the water level has dropped such that it is more difficult for the water to be ejected. This is thought to relate to the welded joint on the TP

where the AGR cladding meets the tube. This also allows ST to begin to rise more rapidly as the ST TC is attached to the cladding section.

1300-end. The test is ended just after 1300 s and the vessel is brought to atmospheric pressure. This leads to a sharp rise in VT and ST. VT and ST drop again as the vessel lid is removed and the TP is removed.

4.2. Flowed Gas Drying Data Plot

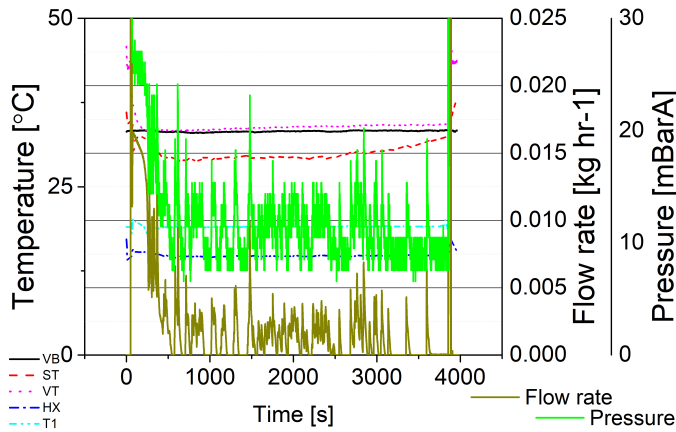
A typical data plot for 60°C AP FGD test is shown in fig. 7. The ST clearly rises with time. A shoulder is clearly visible in ST around 250 s when the gas backfills have been completed and the pump speed was set. The flow rate fluctuates somewhat with time and in places it would seem that these fluctuations can be paired with changes in pressure and TC readings but this is far from certain.

All FGD plots were broadly similar in this behaviour and provided limited information as to what was happening.

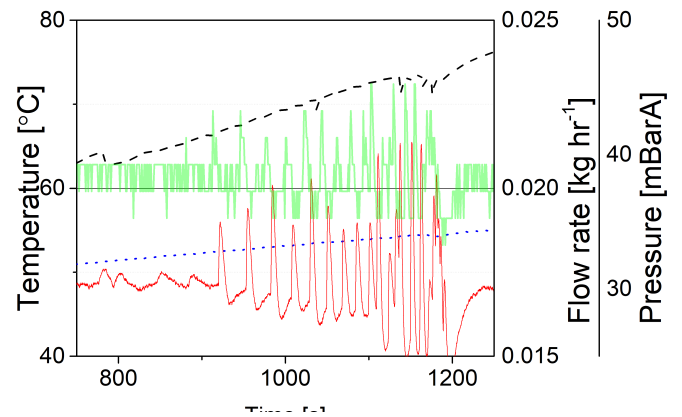
4.3. Results of Initial Drying Tests

The maximum rate for each of the 36 conditions used is shown in table 1. It is clear that that 150°C vacuum drying is by far the most effective method with values between 35 and 50 mg min⁻¹. 60°C vacuum and 150°C ambient pressure drying are next most effective at 12.5-16.6 mg min⁻¹. In almost all cases the type of gas used had no noticeable impact, the exception being 150°C high pressure drying where air and nitrogen were considerably higher than argon and carbon dioxide. This is thought to be due to the greater volumetric flow rates achieved with these gases due to the lower gas density.

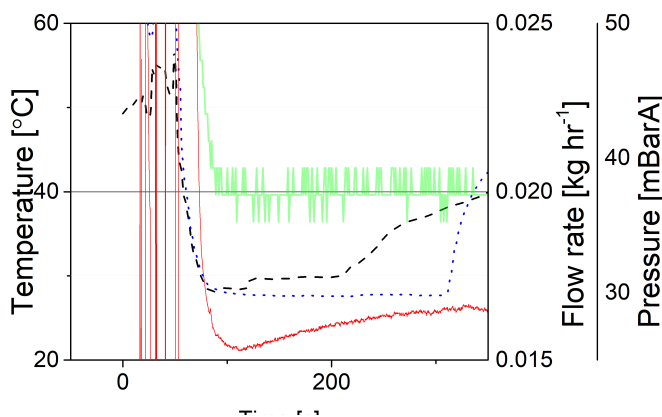
Figure 8 shows the variation in drying rates for different tests during the first set of drying tests (discussed above) and the second set (discussed below). The first set of drying tests (Hot Vac 1, Warm Vac 1 and Hot AP 1) seem to show that the Hot vacuum conditions produce more variation even allowing for the greater number of tests in these conditions. This was attributed to difficulties in consistently controlling temperature and errors introduced when carrying out gas flushes.



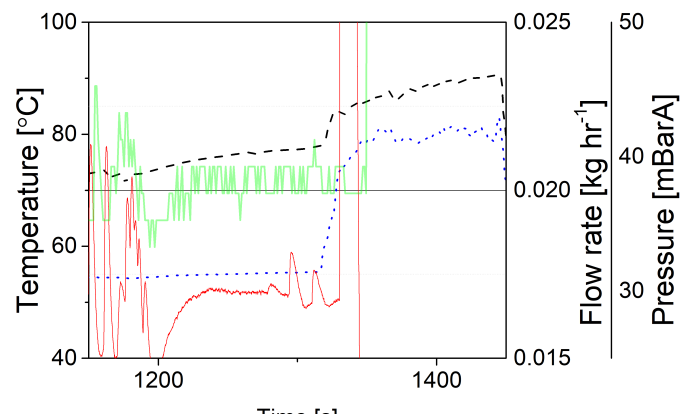
(a) Full test data.



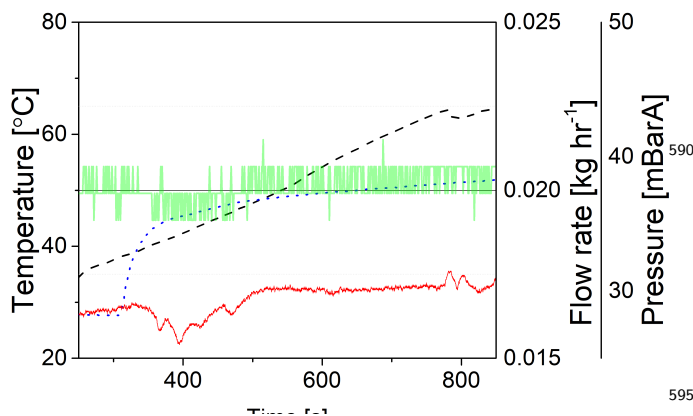
(d) 800-1200 seconds.



(b) 0-300 seconds.



(e) 1200 seconds-end.



(c) 300-800 seconds.

Figure 6: Typical data plot for initial vacuum drying tests.

- The heat tracing that had been used was not suitable.
- The gas pump was found to produce fluctuations and regularly tripped out. This was due to the pump controller which was later replaced with a new model.
- In FGD it was difficult to obtain the required inlet gas temperature for 150°C drying. This was attributed to low flow rates (low heat transfer) and the length/mass of SS pipework between the circulation heater and vessel (heat loss).
- No water was collected in the condenser since the cooling water temperature was above the dew point. This led to the molecular sieve being overwhelmed and water condensing out into the vacuum pump oil.

4.4. Learning Points from Initial Testing

The initial tests brought to light several issues;⁵⁹⁰

- Minor differences in the starting temperature appeared to have a significant impact on overall drying rate.
- The gas flushes were thought to exacerbate this.⁶⁰⁵

585

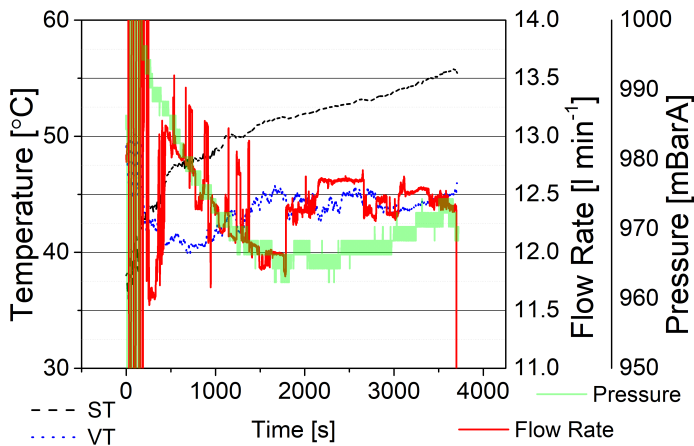


Figure 7: Typical data plot for flowed gas drying.

		11 BarA	1 BarA	20 mBarA
CO ₂	RT	0	0	0
	150°C	0.15	0.5	15
	60°C	2.96	12.5	42.5
Argon	RT	0.34	0.33	0
	150°C	1.02	1.8	15 ⁶²⁵
	60°C	1.48	16.6	26.6
air	RT	0	0	0.33
	150°C	0.48	0.71	13.4
	60°C	7.72	15.2	49.5
N ₂	RT	0	0	0 ⁶³⁰
	150°C	0.82	0.34	15.2
	60°C	13.6	16.4	35

Table 1: Maximum drying rates under different conditions.

- Heel water complicated the system with little benefit. It could be removed easily and obscured more interesting data.

4.5. Initial Minor Changes

For some of the later FGD tests the pipework was changed so that the hose from the circulation heater went directly to the vessel. This was found to have some improvement by reducing the length of pipework from which heat could be lost but the temperature was still somewhat below what had

Since the gas being used seemed to have little impact a decision was made to repeat the 60°C and 150°C vacuum drying tests using air and therefore eliminating the need to carry out gas flushes.

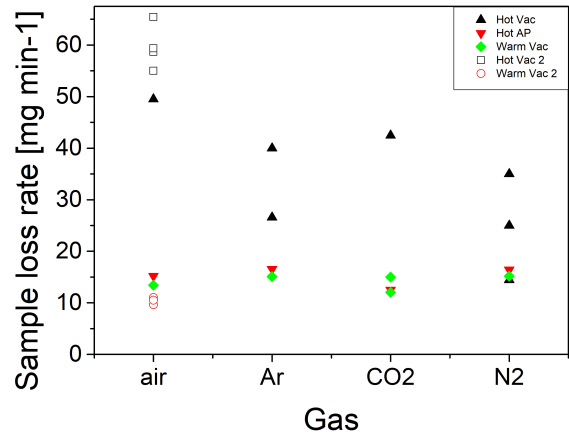


Figure 8: Variation in drying rates for different tests.

Finally ice was added to the cooling water tank to improve the efficiency of the condenser.

The results of these changes are shown in fig. 8 (Hot Vac 2, Warm Vac 2). The results now show much closer grouping of the data and an increase in drying rate. The 150°C drying tests still show more variation but the variation between tests is greatly reduced. The rates for all of the second set of 150°C vacuum drying tests are greater than that for the first set of tests. This is due to a higher initial starting temperature dictated by a more controlled testing methodology.

It was also found that significant quantities of water could now be collected from the condenser. By recording the mass change of the molecular sieve it was also found to be possible to carry out a mass balance for the water loss which accounted for all of the water (within the limits imposed on measurements).

5. First Modifications

Having completed the initial drying tests above the rig was now reconfigured based on some of the issues found. The updates to drying rig are shown in fig. 4. The most significant change was the movement of the flowmeter. The flow meter was initially placed beyond the condenser to prevent gas above the flow meter operating temperature causing damage. After the initial tests it was clear that the gas temperature would not exceed

650 the operating temperature so could be safely fitted upstream of the condenser where more precise measurements could be found.

Since the pipework was being modified, redundant pipework (primarily from the removal of the DPM) was removed where possible, however to simplify construction process several lengths of unnecessary pipework were left in place but blanked. These did however allow temporary instruments to be fitted during early testing.

660 One of the major concerns was related to the flow rate and reliability of the pump. The manufacturers informed us they were aware of the issue and in the process of designing a new controller. To allow this the rig was initially constructed without the recirculation pipework for FGD with these lines blanked after valves which had originally been fitted to isolate this line during vacuum drying.

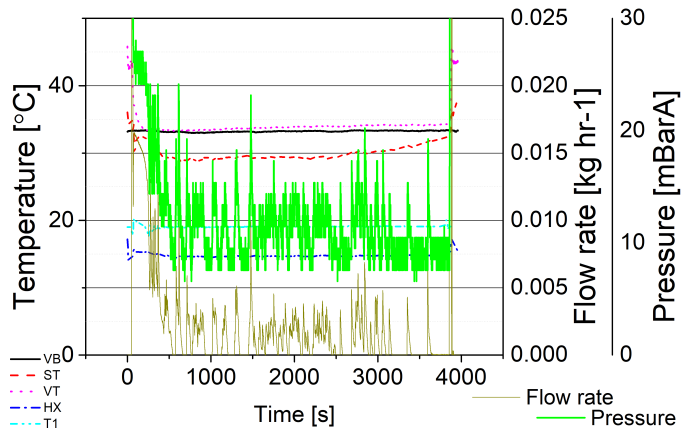
670 An additional TC was fitted to the base of the drying vessel (VB) to give a further indication of the temperature of the vessel walls at the base.

Initial commissioning following the first modifications found that the ultimate pressure recorded was less than 3 mBarA which was considerably lower than the 20 mBarA that had previously been obtainable. The lower pressure resulted in lower dew point so the condenser was no longer able to condense out any water despite the use of iced water, however a mass balance could be achieved through the mass change in the molecular sieve although with some difficulty.

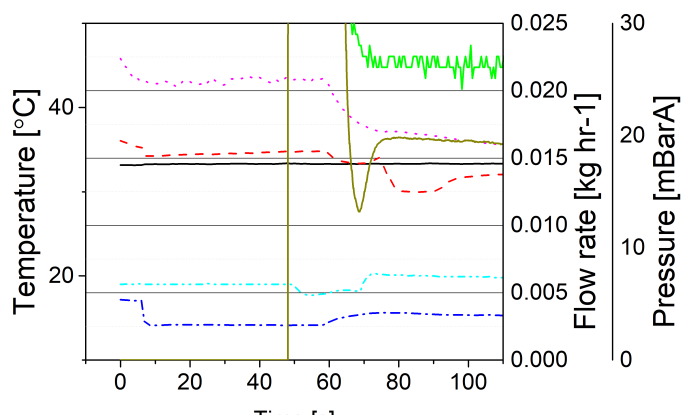
685 The use of heel water was abandoned for multiple reasons. It was found that heel water could be removed with relative ease and as such little was learnt from it's inclusion. It also complicated the data plots and potentially hid more useful data relating to trapped water. Also with the reduced pressure making the water cooled condenser ineffective the molecular sieve was quickly overwhelmed so reducing the quantity of water being removed was beneficial.

5.1. Modified Rig Vacuum Drying Data

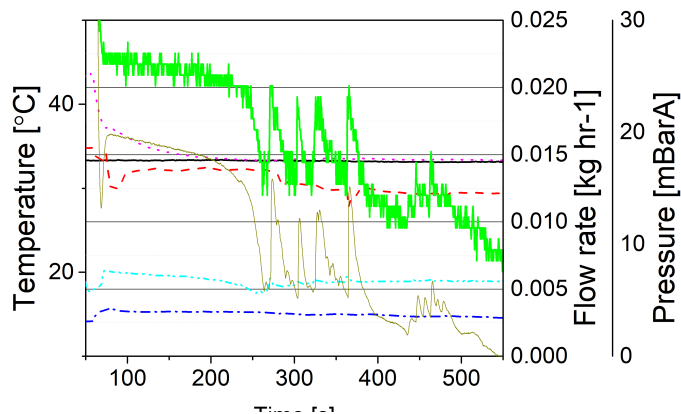
690 Figure 9 shows a typical data plot for the modified rig when vacuum drying. The key difference between this test and that shown in fig. 6 is the



(a) Full test data.



(b) 0-100 seconds



(c) 100-500 seconds.

700 quantity of water within the test piece. For this test the TP was full of water (around 7 g), with the exception of an unavoidable air space when the lid was fitted. The vessel heater had been turned on for at least 30 minutes before the test to ensure that the wall temperature had stabilised. Multiple large scale plots for fig. 9 are available in the addendum.

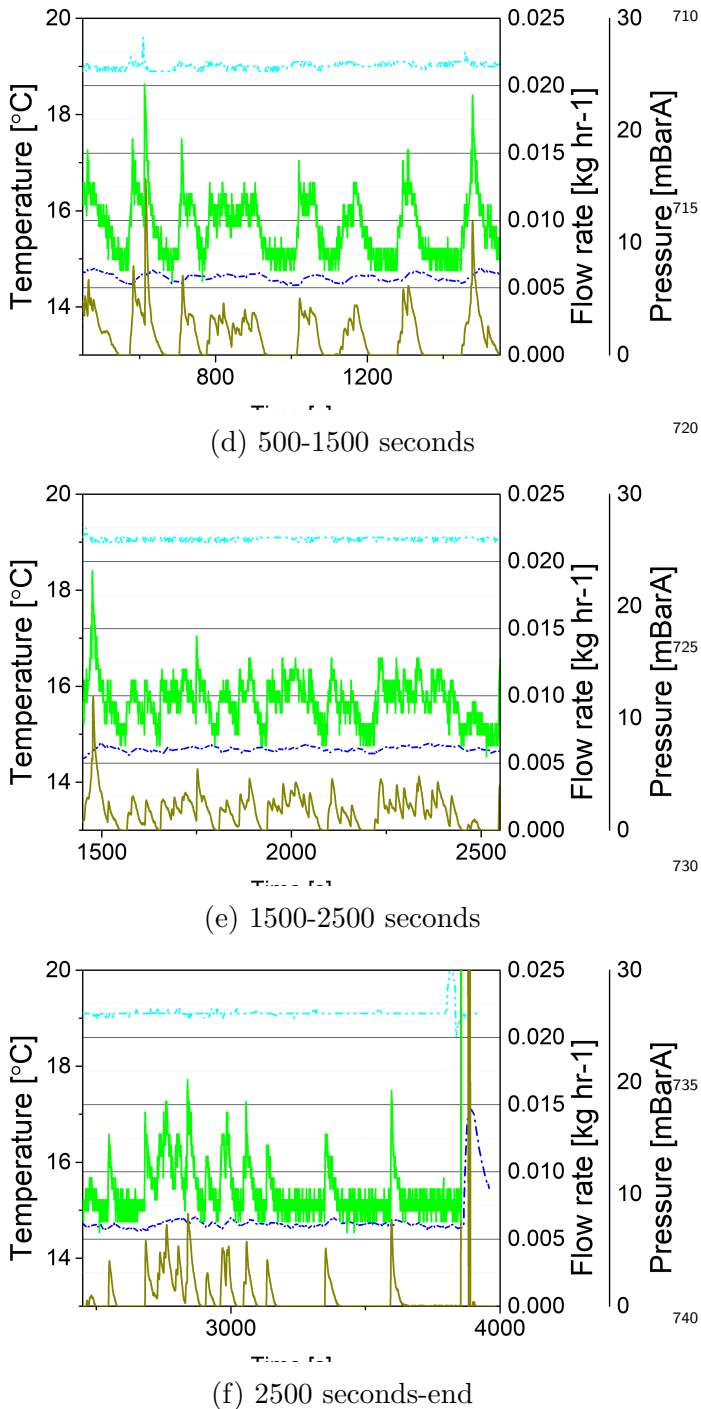


Figure 9: Typical data plots for vacuum drying tests after rig modification.

0-100 seconds. Upon its initial evacuation the flow rate spikes and then drops away. The pressure begins to stabilise around 26 mBarA giving a boiling point of water of around 22°C. T1 and VT initially drop due to adiabatic cooling. As the warm air removed from the vessel passes T1 and HX they

rise.

The vessel is evacuated leading to a drop in flow rate down to a minima. As the vessel is evacuated a jet of water is forced from the pinhole which is below the water level in the TP as the airspace expands. This water then begins to boil upon contact with the vessel as VB is recorded as 33°C. This leads to an increase in flow rate which then levels out.

100-500 seconds. The water ejected from the TP boils away leading to a drop in flow rate and pressure. ST also drops as the heat is used boil the ejected water.

500-1500 seconds. Throughout this period there are large spikes in flow rate from below the level of detection with each spike accompanied by a spike in pressure. This is believed to be due to small drops of water being ejected from the pinhole as it boils. These spikes also lead to slight rises in T1 and HX as does ST.

1500-2500. Similar behaviour to 500-1500 seconds but with smaller but more frequent spikes in flow rate and pressure accompanied by spikes in Vout and HX but ST remains relatively constant.

2500-4000 seconds. Spikes in pressure and flow rate become less frequent as the level of water drops away. ST begins to rise.

5.2. Overall Vacuum Drying Rate

In fig. 10 the change in overall drying rate as a function of the mass of water in the TP is shown. When the TP is full the rate is considerably higher than when it has been reduced to containing only 4 g of water. Below 4 g there is very little variation in the drying rate despite the fact that this is the region that showed considerable variation during initial testing. This would suggest that the modifications, both physical and operational have greatly increased the confidence and reliability of the data obtained.

5.3. Modified Rig Flowed Gas Drying Data

The second tranche of drying tests was carried out using the new pump controller. During

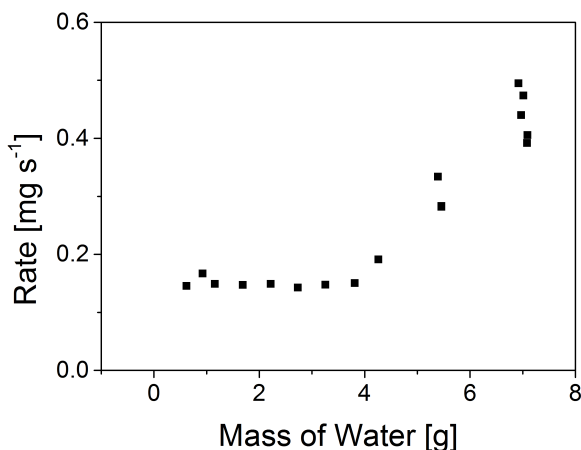


Figure 10: Drying rate at different masses of trapped water for the second tranche of vacuum drying tests.

the second tranche of vacuum drying tests it was decided that it would be possible to safely reintroduce a DPM for the second tranche of FGD tests. A Michell SF52 DPM was now used with a range of -40°C to $+60^{\circ}\text{C}$. It was fitted adjacent to the Vout TC.

5.4. FGD 2

A data plot from the second tranche of FGD drying is shown in fig. 11. This was carried out in identical conditions to the the 60°C AP tests in the initial tests.

The overall drying rate was found to be 0.01 mg s^{-1} which is of the same magnitude to that found in the initial tests. The dew point drops initially as the air dries levelling out at -40°C which is the lower limit of the instrument. It then begins to fluctuate between -40°C and -38°C indicating that water is beginning to be removed from inside the TP.

The pressure within the system can be seen to increase and decrease in line with the cycling of the circulation heater and this in turn affects the flow rate. Within this general behaviour there does however appear to be some minor fluctuations which match the fluctuations in dew point.

Once again the pressure and flow rate data seem to provide limited information since they are influenced by the cycling of the circulation heater. On the whole the data is more stable than before the modifications and as a result it is felt that

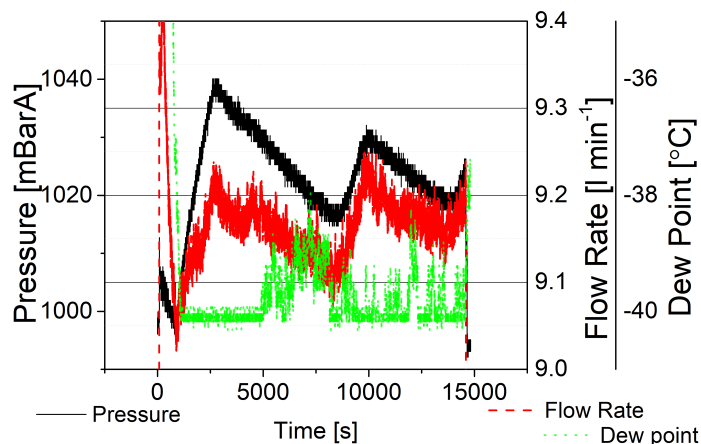


Figure 11: Plot of FGD after initial rig modifications.

useful data may be obtainable from temperature and dew point data.

6. Conclusions

While the drying of spent nuclear fuel has been undertaken for over three decades little systematic research as been undertaken to compare the two drying methods commonly used. This paper has described the development of a rig that it is hoped will be able to provide clear evidence of the most effective method. While the emphasis and driving force has been to find a method for drying SS clad AGR fuel there is no reason that the learnings can not be applied to other fuel types or indeed other specialist drying applications. Furthermore it is hoped that this rig will allow different methods of online measurement to be examined to see how parameters such as pressure, temperature and flow rate may be used to analyse the behaviour within a sealed canister in real time.

The initial work has shown that vacuum drying appears to be considerably more effective than FGD. While the two sets of tests produce roughly the same results in terms of the drying rates observed the improvements made to the rig have greatly reduced the test to test variation.

The tests carried out so far have shown that minor temperature changes can be detected when vacuum drying which may be used to infer what is happening within the drying vessel. Similarly

variations in the flow rate, pressure and dew point may also prove useful. Work with the drying rig will continue to try and assess the whether any of these parameters may be measured in sufficient detail to be if any practical benefit.

Several further changes are planned including a flow meter with a lower limit of detection and the addition of energy metering to allow the relative cost of each drying method to be assessed.

Acknowledgements

The authors would like to thank the EPSRC for student funding and the National Nuclear Laboratory and Nuclear Decommissioning Authority for funding the drying rig construction.

References

- [1] N. Brittain, EDF Energy - Nuclear Generation The AGR Design, Fukushima and More (Feb. 2012). URL www-diva.eng.cam.ac.uk/mphil-in-nuclear-energy/external-lectures/2011-12-lectures/edf-energy-ng-cambridge-09022012.pdf/at_download/file
- [2] J. Best, W. Stephen, A. Wickham, Radiolytic graphite oxidation, *Progress in Nuclear Energy* 16 (2) (1985) 127–178. doi:10.1016/0149-1970(85)90002-2. URL <http://www.sciencedirect.com/science/article/pii/0149197085900022>
- [3] W. A. England, M. J. Bennett, D. A. Greenhalgh, S. N. Jenny, C. F. Knights, The characterization by raman spectroscopy of oxide scales formed on a 20cr\25ni\Nb stabilized stainless steel, *Corrosion Science* 26 (7) (1986) 537–545. doi:10.1016/0010-938X(86)90021-1. URL <http://www.sciencedirect.com/science/article/pii/0010938X86900211>
- [4] J. Kyffin, Technological Development to Support a Change in the United Kingdom's Strategy for Management of Spent AGR Oxide Fuel, in: *Proceedings of the International Conference on Management of Spent Fuel from Nuclear Power Reactors*, IAEA, Vienna, 2015.
- [5] D. Hambley, Technical Basis for Extending Storage of AGR Fuel, Salt Lake City, 2013. URL https://www.researchgate.net/profile/David_Hambley/publication/279058579_Technical_Basis_for_Extending_Storage_of_the_UK's_Advanced_Gas-Cooled_Reactor_Fuel/links/558932230aed6bff80b421d.pdf
- [6] Intergranular Corrosion. URL <https://www.nace.org/Corrosion-Central/Corrosion-101/Intergranular-Corrosion/>
- [7] A. Al-Shater, D. Engelberg, S. Lyon, C. Donohoe, S. Walters, G. Whillock, A. Sherry, Characterization of the stress corrosion cracking behavior of thermally sensitized 20cr-25ni stainless steel in a simulated cooling pond environment, *Journal of Nuclear Science and Technology* 0 (0) (2017) 1–10. doi:10.1080/00223131.2017.1309305. URL <http://dx.doi.org/10.1080/00223131.2017.1309305>
- [8] S. M. Bruemmer, E. P. Simonen, P. M. Scott, P. L. Andresen, G. S. Was, J. L. Nelson, Radiation-induced material changes and susceptibility to intergranular failure of light-water-reactor core internals, *Journal of Nuclear Materials* 274 (3) (1999) 299–314. doi:10.1016/S0022-3115(99)00075-6. URL <http://www.sciencedirect.com/science/article/pii/S0022311599000756>
- [9] E. A. Little, Development of radiation resistant materials for advanced nuclear power plant, *Materials Science and Technology* 22 (5) (2006) 491–518. doi:10.1179/174328406X90998. URL <http://0-www.maneyonline.com.wam.leeds.ac.uk/doi/abs/10.1179/174328406X90998>
- [10] C. Taylor, INIS Repository Search - Single Result, in: *Proceedings of the Radiation-induced Sensitisation of Stainless Steels*, Berkeley, UK, 1986. URL <https://inis.iaea.org/search/searchsinglerecord.aspx?recordsFor=SingleRecord&RN=18098354>
- [11] J. Kyffin, The technical case for interim Storage of AGR fuel and development of a programme of further work, IChemE, Manchester, 2014.
- [12] Nuclear Decommissioning Authority, Oxide Fuels - Preferred Option - Publications - GOV.UK, Tech. Rep. SMS/TS/C2-OF/001/Preferred Option (Jun. 2012). URL <https://www.gov.uk/government/publications/oxide-fuels-preferred-option>
- [13] R. Sindelar, D. Vinson, N. Iyer, D. Fisher, Overview of Criteria for Interim Wet and Dry Storage of Research Reactor Spent Nuclear Fuel, Tech. rep., SRS (2010). URL <http://sti.srs.gov/fulltext/SRNL-STI-2010-00688.pdf>
- [14] J. Morris, S. Wickham, P. Richardson, C. Rhodes, M. Newland, Contingency Options for the Dry Storage of Magnox Spent Fuel in the UK, in: *Proceedings of the 12th International Conference on Radioactive Waste Management and Environmental Remediation*, ICEM, Vol. 1, Liverpool, 2009, pp. 817–823. doi:10.1115/ICEM2009-16331.
- [15] NRC: Dry Cask Storage. URL <https://www.nrc.gov/waste/>

spent-fuel-storage/dry-cask-storage.html

920 [16] X. L. Yan, R. Hino (Eds.), Nuclear hydrogen production handbook, Green chemistry and chemical engineering, Taylor & Francis, Boca Raton, FL, 2011.

[17] ASTM, Guide for Drying Behavior of Spent Nuclear Fuel, Tech. Rep. C-1553, ASTM International (2008). URL <http://www.astm.org/Standards/C1553.htm>

925 [18] W. S. Large, Review of Drying Methods for Spent Nuclear Fuel, Tech. Rep. WSRC-TR-97-0075, Savannah River Site (US), Aiken, SC 29808 (Oct. 1999). URL <http://www.osti.gov/scitech/biblio/14490>

930 [19] W. Kupferschmidt, M. Stephens, AECL's Waste Management and Decommissioning Program, Australian Nuclear Association, 2006, p. 685.

[20] G. E. Culley, Hanford's Progress Toward Dry Interim Storage of K Basin's Spent Fuel, Tech. Rep. WHC-SA-3107-FP; CONF-960804-, Westinghouse Hanford Co., Richland, WA (United States) (May 1996). URL <http://www.osti.gov/scitech/biblio/330736>

935 [21] D. Cox, I. Bainbridge, K. Greenfield, Management of Legacy Spent Nuclear Fuel Wastes at the Chalk River Laboratories: Operating Experience and Progress Towards Waste Remediation, in: Proceedings of WM'05 Conference, Tucson, Az, 2005.

940 [22] P. G. Loscoe, Transitioning Metallic Uranium Spent Nuclear Fuel from Wet to Dry Storage, in: WM 2000 Proceedings, Tucson, Az, 2000. URL <https://www.wmsym.org/archives/2000/pdf/54/54-9.pdf>

945 [23] A. L. Pajunen, Cold Vacuum Drying Residual Free Water Test Description, Tech. Rep. HNF-1851, Fluor Daniel Hanford Inc., Richland, WA (United States) (Dec. 1997). URL <http://www.osti.gov/scitech/biblio/10148296>

950 [24] R. E. Lords, W. E. Windes, J. C. Crepeau, R. W. Sidwell, Drying Studies of Simulated Doe Aluminum Plate Fuels, Tech. Rep. INEL95/00437; CONF-960611644, Idaho National Engineering Lab., Idaho Falls, ID (United States) (May 1996). URL <http://www.osti.gov/scitech/biblio/236247>

955 [25] R. E. Lords, W. E. Windes, J. C. Crepeau, R. W. Sidwell, Drying Studies for Corroded Doe Aluminum Plate Fuels, Tech. Rep. INEL96/00134; CONF-96080429, Idaho National Engineering Lab., Idaho Falls, ID (United States) (May 1996). URL <http://www.osti.gov/scitech/biblio/260992>

960 [26] L. Rodrigo, L. Therrien, B. Surette, Low-Temperature, Vacuum-Assisted Drying of Degraded Spent Nuclear Fuel, in: Waste Management, Decommissioning and Environmental Restoration for

970

Canada's Nuclear Activities Current Practices and Future Needs, Canadian Nuclear Society, Ottawa, 2005.